Synthetic gene circuits enable systems-level biosensor discovery at the host-microbe interface

Running title: Synthetic gene circuits enable gut biosensor discovery

Authors

Alexander D Naydich[1,2], Shannon N Nangle[1,2], Johannes J Bues[1], Disha Trivedi[1], Nabeel Nissar[1], Mara C Inniss[1], Matthew J Neiderhuber[1], Jeffrey C Way[2], Pamela A Silver[1,2]# & David T Riglar[1,2]#

Affiliations

1. Department of Systems Biology, Harvard Medical School, Boston, MA 02215
2. Wyss Institute for Biologically Inspired Engineering, Boston, MA 02215

Corresponding author email: David_Riglar@hms.harvard.edu and Pamela_Silver@hms.harvard.edu

Abstract word count: 348

Text word count (excluding the references, table footnotes, and figure legends): 4912

Present addresses: J.J.B.: Laboratory of Systems Biology and Genetics, EPFL-SV-IBI-UPDEPLA, Station 19, AI 1240, CH-1015 Lausanne, Switzerland; N.N.: Littleton MA, 01460; M.C.I.: Obsidian Therapeutics, 1030 Massachusetts Avenue, Suite 400, Cambridge MA, 02138; M.J.N.: McKay Lab at UNC Chapel Hill, 3344 Genome Sciences Building, Campus Box 3280, Chapel Hill, NC 27599.

ABSTRACT

The composition and function of the gut microbiota are strongly associated with human health, and dysbiosis is linked to an array of diseases, ranging from obesity and diabetes to infection and inflammation. Engineering synthetic circuits into gut bacteria to sense, record and respond to *in vivo* signals is a promising new approach for the diagnosis, treatment and prevention of disease. Here, we repurpose a synthetic bacterial memory circuit to rapidly screen for and discover new *in vivo*-responsive biosensors in commensal gut *Escherichia coli*. We develop a pipeline for rapid systems-level library construction and screening, using next-generation sequencing and computational analysis, which demonstrates remarkably robust identification of responsive biosensors from pooled libraries. By testing both genome-wide and curated libraries of potential biosensor triggers—each consisting of a promoter and ribosome binding site (RBS)—and using RBS variation to augment the range of trigger sensitivity, we identify and validate triggers that selectively activate our synthetic memory circuit during transit through the gut. We further identify biosensors with increased response in the inflamed gut through comparative screening of our libraries in healthy mice and those with intestinal inflammation. Our results demonstrate the power of systems-level screening for the identification of novel biosensors in the gut and provide a platform for disease-specific screening using synthetic circuits, capable of contributing to both the understanding and clinical management of intestinal illness.

IMPORTANCE

The gut is a largely obscure and inaccessible environment. The use of live, engineered probiotics to detect and respond to disease signals *in vivo* represents a new

frontier in the management of gut diseases. Engineered probiotics have also shown promise as a novel mechanism for drug delivery. However, the design and construction of effective strains that respond to the *in vivo* environment is hindered by our limited understanding of bacterial behavior in the gut. Our work expands the pool of potential biosensors for the healthy and diseased gut, providing insight into host-microbe interactions and enabling future development of increasingly complex synthetic circuits. This method also provides a framework for rapid prototyping of engineered systems and for application across bacterial strains and disease models.

50 **INTRODUCTION**

51 Recent advances in our understanding of both the human microbiota and
52 biological engineering techniques have created myriad possibilities for the development
53 of synthetic microbes for *in vivo* clinical applications (1, 2). Bacteria residing in the gut
54 are uniquely positioned to monitor a variety of host, microbial, and environmental factors
55 and to respond to changes in intestinal homeostasis. Engineered gut bacteria also offer
56 the potential for *in vivo* production and delivery of therapeutics (2).

57 Environment- and disease-responsive functions, which could minimize both the
58 metabolic burden of engineered systems on the bacteria and off-target effects on the
59 patient, offer exciting prospects for clinical applications. To this end, recent *in vivo*
60 approaches have developed sensors responding to inflammation (3, 4), intestinal
61 bleeding (5), and pathogen quorum-sensing systems (6, 7). However, the construction
62 of disease-responsive circuits in bacteria has been hindered by the limited number of
63 characterized bacterial systems that can be reliably employed as sensors.

64 Mining the genomes of native gut bacteria is a promising approach for
65 discovering new sensors that respond under conditions of interest, such as in the
66 healthy or diseased gut. To date, these efforts have largely relied on transcriptome
67 sequencing and proteomics of fecal samples. However, to obtain an instantaneous
68 snapshot of bacterial behavior inside the gut using these techniques, invasive sampling
69 is required (i.e., colonoscopy and biopsy). Furthermore, transient or low-abundance
70 signals may not be detected, and any responsive genetic elements identified with these
71 techniques may not function predictably when employed in synthetic circuits.
72 Approaches such as *in vivo* expression technology (IVET) and recombinase-based

IVET (RIVET) have also been used to track *in vivo*-expressed genes non-invasively, but detect only constitutive expression (for IVET) and may have high false-positive rates (8). Nevertheless, these technologies show the potential for systems-level approaches to interrogate the behavior of the microbiota.

We have previously developed an approach for non-invasive measurement of bacterial responses in the gut, based on a robust synthetic memory circuit, which records environmental stimuli via a transcriptional trigger (3, 9). When activated, the trigger turns on a memory switch, which can retain the memory-on state for over a week in the gut (9). After the bacteria pass through the host, their memory state can be determined via reporter gene expression, enabling non-invasive readout of transient signals within the gut. The circuit can maintain functional and genetic stability during six months' colonization of the mouse gut, demonstrating its suitability for longitudinal studies and its potential to support the development of stable, engineered biosensors for *in vivo* deployment (3).

Here, we adapt this memory circuit for parallel, high-throughput screening of hundreds of potential triggers. We apply this method to identify new biosensors responding specifically to the *in vivo* gut environment. Through comparison between healthy mice and those suffering from inflammation, we also identify triggers that respond differentially during disease. Together, these results provide a platform for *in vivo* non-invasive biosensor discovery and longitudinal testing.

RESULTS

95 **Bacterial memory as a biosensor screening tool.** To enable screening of new
96 potential biosensors in parallel, we modified our previously-developed *E. coli* memory
97 circuit, which is based on the λ phage lysis–lysogeny switch (Fig. S1A) (9). This
98 modified circuit is referred to as the high-throughput memory system (HTMS) (Fig. 1A).
99 Both the original memory circuit and the HTMS consist of a trigger—based on a
100 transcriptional promoter activated in the presence of a certain stimulus—and a memory
101 switch. The memory-on and memory-off states of the switch correspond to the mutually-
102 repressive proteins Cro and CI, respectively. Additionally, a β-galactosidase (LacZ)
103 reporter is produced in the memory-on state.
104 One key modification for the HTMS is the triggering of memory using a dominant-
105 negative mutant of the *cI* gene (*cIDN*), instead of *cro* used in the original trigger. When
106 the trigger promoter is activated by a stimulus, CIDN monomers, which have an N55K
107 mutation in the DNA binding region (10) dimerize with wild-type (WT) CI monomers
108 expressed in the memory-off state, creating heterodimers that are deficient in DNA-
109 binding. This leads to derepression of P_R and transition to the memory-on state. As with
110 the CI used in the memory element, CIDN carries a mutation to prevent RecA-mediated
111 cleavage (ind-) (11).
112 Use of CIDN in the trigger ensures that there is no delay of switching to the
113 memory-on state in the case of high, or constant, expression of the trigger promoter. To
114 test this, a P_{tet} trigger driving *cIDN* or *cro* was integrated into *E. coli* K-12 MG1655 and
115 NGF-1 strains containing a memory element. When grown in the presence of a high
116 concentration (100 ng/ml) of anhydrotetracycline (aTc) inducer, *cIDN*-triggered strains

117 showed switching to the memory-on state, while *cro*-triggered strains switched only after
118 a subsequent period of growth in the absence of aTc (Fig. 1B).
119 The original memory circuit expresses a *lacZ* reporter gene for screening on
120 indicator plates (9). To analyze pooled libraries containing many strains with varied
121 trigger promoters, the HTMS also expresses a spectinomycin-selectable resistance
122 gene (*aadA)* in the memory-on state.
123 This antibiotic-selectable memory maintains response characteristics similar to
124 the original memory element. To test this, a P_{tet} trigger driving *cIDN* was integrated into
125 strains containing *lacZ* (original) or *aadA*+*lacZ* (HTMS) memory elements, creating
126 PAS809 and PAS810, respectively (see Table 1 for strain list). Strains were induced by
127 aTc (0-100 ng/ml) and the response quantified by plating cultures on indicator plates
128 containing 5-bromo-4-chloro-3-indolyl-β-d-galactopyranoside (X-gal), which turns blue in
129 the presence of LacZ, indicating a memory-on state (Fig. S1B). Both strains responded
130 similarly to aTc (*original memory* EC50: 4.1-4.6 ng/ml, 95% CI; *HTMS* EC50: 4.0-4.3
131 ng/ml, 95% CI), confirming the circuit's modularity to additional reporters in the memory-
132 on state.
133 The HTMS allows faithful selection of memory-on colonies with spectinomycin
134 treatment. Plating of fully memory-off, fully memory-on, and 50-50 mixed cultures of
135 PAS810, on indicator plates with and without spectinomycin further demonstrated that
136 all spectinomycin-selected colonies were also *lacZ* positive (Fig. 1C). Spectinomycin did
137 not yield false-positive results by inducing memory switching (fully memory-off: 0% +/-
138 0% SE, n = 8), nor excessive false-negative results through inhibition of memory-on
139 bacterial growth (fully memory-on: 93.0% +/- 4.2% SE, n = 8; 50-50 mix: 49.7% +/- 1.5%

140 SE, n = 5) (Fig. 1C). Together these results demonstrate the ability of the HTMS to
141 measure biosensor response and allow selection for downstream pooled analyses.
142 **Biosensor library construction.** To build biosensor libraries for genomic
143 integration, we adapted a Tn7 transposon genome insertion plasmid (12) for rapid
144 Golden Gate assembly (13) of bacterial promoters upstream of the *cIDN* trigger and
145 insertion into the genome of memory bacteria (Fig. 2A and S2). The modularity of this
146 cloning strategy allows for adjustment of trigger sensitivity through incorporation of
147 ribosomal binding site (RBS) variants, which vary the translation rate of mRNA
148 transcripts (Fig. 2A). To test this concept, triggers consisting of a P_{tet} promoter
149 combined with nine synthetic RBS sequences—previously demonstrated to vary widely
150 in their translation strength (14) (Fig. 2A)—were constructed and inserted into the
151 genome of HTMS bacteria, and the HTMS response to varying concentrations of aTc
152 (0-100 ng/ml) was characterized (Fig. 2B). The RBS variants differed in their extent of
153 memory induction at 0.1-10 ng/ml aTc (EC50 ranging from 0.5 to 4.1 ng/ml for
154 responsive strains), illustrating our ability to tune trigger sensitivity.
155 We explored two approaches for generating biosensor libraries: 1) a genome-
156 wide collection of trigger promoters that would enable screening of a bacterium's entire
157 range of transcriptional responses (MG1655 library), and 2) a curated collection of
158 promoters with sensitivity variants aimed at detecting inflammation (Nissle 1917 library).
159 Both libraries were assembled into an HTMS-containing *E. coli* NGF-1 strain (PAS811),
160 as NGF-1 has proven to be an efficient and persistent colonizer in the mouse gut (3, 9,
161 15). The genome-wide library was sourced from a previously published collection of
162 1600 unique promoters from *E. coli* K-12 MG1655 (16). Promoters and their wild-type

163 RBSs were amplified by PCR from this collection, assembled into our transposon
164 plasmid, and integrated as triggers into the genome of PAS811. Because our method
165 focuses on detecting off-to-on sensor transitions, the resultant library was further
166 subsampled by pooling 500 colonies that were LacZ-negative under routine *in vitro*
167 culture. Sequencing confirmed the presence of 155 unique strains in this final genome-
168 wide library.

169 Our second library was constructed with a subset of promoters sourced from the
170 human probiotic *E. coli* Nissle 1917, which are involved in anaerobic respiration of
171 sulfur- or nitrogen-oxides or nitrate, produced by the gut epithelium during inflammation
172 (17, 18). For each promoter, a trigger with its wild-type RBS, as well as with five
173 different synthetic RBSs (MCD5, MCD10, MCD15, MCD17 and MCD23) (14) were
174 included to tune sensitivity. Sequencing confirmed that the assembled library contained
175 61 unique strains out of 66 total designed constructs.

176 **Parallel analysis faithfully reports biosensor response.** To screen for
177 biosensor response, HTMS libraries are exposed to a condition of interest (Fig. 3A), and
178 put through a processing, sequencing and analysis pipeline (Fig. 3B). After exposure,
179 HTMS bacteria are recovered and cultured. The initial culture is split into two and back-
180 diluted, and one of the two new cultures is subjected to spectinomycin selection.
181 Following selection, the trigger regions of both cultures are sequenced and analyzed to
182 produce an odds ratio for each trigger promoter in the library, corresponding to that
183 trigger's memory state. To calculate odds ratios, results are normalized to a positive
184 normalization strain (PAS812) which remained in a memory-on state (Fig. 3B).

185 Pooled library analysis is predictive of the on/off state of HTMS bacteria. The
186 Nissle 1917 library was cultured aerobically in liquid media and analyzed to obtain odds
187 ratios as described above. Concurrently, individual strains from this library were grown
188 on indicator plates to assess each strain's *in vitro* memory state directly. Both tests
189 showed strong agreement, with strains that were LacZ-positive also displaying higher
190 odds ratios (Fig. 3C). Receiver operating characteristic analysis confirmed efficient
191 distinction between memory-on and memory-off states, with an odds ratio of
192 approximately 0.02 delimiting the boundary (Fig. 3D). This confirmed our sequencing
193 method as a reliable indicator of biosensor memory state.

194 **Differential biosensor response in the healthy mouse gut.** To screen for
195 biosensor response to growth within the murine gut, the MG1655 library was
196 administered to specific-pathogen free (SPF) mice by oral gavage (~10^7
197 bacteria/mouse), and fecal samples were collected over one (n=2) or seven (n=3) days.
198 High library diversity was maintained in both experiments (92% and 82% of strains
199 identified in gavage samples present at experiment endpoint, respectively). Analysis of
200 HTMS strains recovered from gavage suspension and fecal samples identified 23
201 unique strains that responded specifically to growth within the gut (gavage: odds ratio <
202 0.02; fecal samples: ≥ 1 timepoint odds ratio ≥ 0.02 and $p < 0.05$) (Fig. 4A and 4B; Data
203 Set S1 and S2). Five strains (containing ydiL, ydjL, gatY, gcvA and ubiG triggers) were
204 detected in the memory-on state in at least 4 of 5 mice. The two most consistent
205 responders (ydjL and ydiL triggers) were selected for follow-up testing.

206 To validate the response of the ydiL and ydjL triggers during gut transit, memory
207 bacteria containing these triggers (ydiL: PAS813; ydjL: PAS814) or a promoterless *cIDN*

208 gene (negative control: PAS815) were administered to SPF mice as monocultures.
209 Fecal samples were collected and analyzed over the subsequent five days. Culture on
210 indicator plates demonstrated an absence of memory activation in all three strains prior
211 to gavage. However, when recovered from fecal samples PAS813 and PAS814
212 colonies were consistently memory-on, confirming activation during gut transit (at Day 2,
213 PAS813: 51% +/- 8% SE; PAS814: 30% +/- 4% SE; negative control: 0% +/- 0% SE; n
214 = 3 per strain) (Fig. 4C).

215 The Nissle 1917 library was also screened to discover promoters responding in
216 the healthy mouse gut. Testing of the Nissle 1917 library over five days following
217 gavage (~10^7 bacteria/mouse) identified 11 strains that specifically responded to *in vivo*
218 growth (Data Set S3). Ten of these, derived from three unique promoters (*ynfEFGH*,
219 *torCAD*, and *yeaR-yoaG* operons) registered a memory-on state in the majority of
220 timepoints and all mice tested (n=4) (Fig. 4D and 4E). Promoter response was similar
221 during parallel analysis in the inflamed mouse gut (n = 4; see below and Fig. 5 for
222 experimental details), further validating these results (Fig. S3 and Data Set S3).

223 RBS variation to adjust trigger sensitivity affects *in vivo* sensing capacity.
224 Variation in sensor response based on trigger RBS was most notably observed with the
225 *ynfEFGH* promoter: WT, MCD5 and MCD17 RBSs showed no response throughout the
226 screening experiment, whereas MCD10, MCD15, and MCD23 registered as memory-on
227 in 100%, 100% and 94% of timepoints, respectively. (Note: Nissle 1917 library strains
228 are referred to below by an abbreviation consisting of the first gene of the operon from
229 which they are derived and the number of their synthetic RBS. For instance, “ynfE15”
230 denotes the trigger consisting of the *ynfEFGH* promoter with MCD15.) To validate these

231 findings, ynfE15 (PAS816), yeaRWT (PAS817), and ynfEWT (PAS818, used here as a
232 negative control) strains were administered to SPF mice as monocultures, with memory
233 status determined by culture on indicator plates (at Day 2, ynfE15: 99% +/- 1% SE;
234 yeaRWT: 31% +/- 4% SE; ynfEWT: 0% +/- 0% SE; n = 3) (Fig. 4F). Of note, changing
235 the ynfE trigger RBS from WT to MCD15 increased memory-on rate in the gut from 0%
236 to nearly 100%.

237 Together these results demonstrate the ability for HTMS analysis to rapidly
238 identify biosensors *in vivo* and the power of varying trigger sensitivity to tune the
239 strength of biosensor response.

240 ***In vitro* induction of *in* vivo-responding biosensor strains.** The Nissle 1917
241 library includes some promoters with previously characterized induction conditions. We
242 tested induction of *ynfEFGH* promoter trigger memory strains, which derive from an
243 operon known to respond to low nitrate (through repression by phosphorylated NarL),
244 and anaerobic (through FNR activation) conditions (19). When grown anaerobically in
245 rich media, PAS816 (ynfE15), produced a memory response (13.3% +/- 0.7% SE; n =
246 7). With added nitrate (20 mM), or in aerobic conditions, the response was zero (-
247 O_2/+nitrate: 0% +/- 0% SE; n = 3; +O_2/+nitrate: 0% +/- 0% SE; n = 3; +O_2: 0% +/- 0%
248 SE; n = 3) (Fig. 4G), consistent with previous literature reports of *ynfEFGH* promoter
249 behavior (19). Additionally, no response was observed from PAS818 (ynfEWT) in any
250 condition (n = 3), suggesting that it is less sensitive than PAS816 (ynfE15), consistent
251 with our *in vivo* results. In addition to growth in rich media, strains were also cultured
252 anaerobically in cecal contents. As in rich media with no inducer, only ynfE15
253 responded to growth in cecal media (3.7% +/- 0.9% SE; n = 3) (Fig. 4G).

254 **Identification of disease-specific biosensors.** To look for sensors responding
255 differentially to disease, we compared the response of the Nissle 1917 library in healthy
256 mice (n = 4; as previously displayed in Fig. 4D, 4E and S3, and Data Set S3) to a
257 murine intestinal inflammation model (Fig. 5A, 5B and S4, and Data Set S3). After
258 library gavage, SPF mice were provided water containing 4% w/v dextran sulfate
259 sodium (DSS) *ad libitum* for five days, and HTMS analysis was performed on fecal
260 samples throughout. Weight loss (Fig. S4A), colon length reduction at endpoint (Fig.
261 S4B), and increased *E. coli* CFU counts (Fig. S4C) were all consistent with increasing
262 inflammation throughout the experiment. Six strains registered memory-on at more
263 timepoints in the DSS-treated group than in the control group (Fig. 5A and 5B). In
264 particular, the ynfE17 trigger strain (PAS819) responded specifically in DSS-treated
265 mice (control: no response; DSS-treated: 93% of timepoints with odds ratio ≥ 0.02 and p
266 < 0.05) (Fig. 5A and 5B, and Data Set S3).
267 To validate ynfE17 (PAS819) response to inflammation, the strain was
268 administered to SPF mice as a monoculture, after which a subset of the mice was
269 provided water containing 4% DSS. Fecal samples were cultured for memory bacteria
270 on indicator plates for 7 days following gavage. As above, body weights (Fig. S4D),
271 post-dissection colon lengths (Fig. S4E) and CFU counts of HTMS bacteria (Fig. S4F)
272 reflected increased inflammation in DSS-treated mice. Confirming the screen results,
273 ynfE17 showed increased response in DSS-treated mice compared to untreated
274 controls, with the greatest difference between groups at days 6 and 7 (at Day 6, +DSS:
275 24% +/- 9% SE, n= 4; control: 5% +/- 2% SE, n = 8) (Fig. 5C). The strong response of
276 PAS819 in the absence of DSS in one of the control group mice indicates that *in vivo*

277 conditions other than DSS treatment can activate the ynfE17 trigger. *In vitro* anaerobic
278 growth both in rich media and in cecal media did not induce ynfE17 (0 +/- 0% SE; n = 7;
279 0 +/- 0% SE, n = 3, respectively), in contrast to ynfE15 (Fig. 4G), suggesting a lower
280 nitrate threshold for ynfE17 activation and that individual bacteria may experience low
281 nitrate conditions within the inflamed mouse gut.
282

283 **DISCUSSION**

284 Here, we have expanded the use of a robust genetic memory circuit to assess
285 the *in vivo* responses of multiple bacterial sensors in parallel. The original memory
286 circuit (9) was altered to allow off-to-on transitions in the presence of constant induction,
287 and to enable selection of memory-on strains from pooled libraries using spectinomycin.
288 We developed a screening, sequencing and analysis pipeline to efficiently identify *in*
289 *vivo*-responding trigger–RBS combinations. Tests conducted with both genome-wide
290 and curated libraries containing hundreds of sensors demonstrated that our method is
291 an effective, non-invasive way to identify new biosensors responding in the gut. We
292 identified and validated biosensors responding to growth in the healthy mouse gut and
293 preferentially in inflamed conditions. Together, these results demonstrate the power of
294 tuning trigger sensitivity to physiological responses and for the HTMS to assess unique
295 features of the mammalian gut environment *in vivo*.

296 One advantage of our method is its ability to discover sensors that could not be
297 rationally designed based on existing knowledge, presenting an opportunity to apply the
298 rapidly increasing but largely uncharacterized genetic diversity identified through
299 microbiome sequencing. For instance, the two validated healthy-gut sensors from our *E.*

300 *coli* MG1655 library (PAS813 and PAS814) are derived from operons with largely
301 uncharacterized function and regulation. PAS814 is triggered by the promoter of the
302 *ydjLKJIHG* operon, which putatively includes a kinase, a transporter protein, two
303 dehydrogenases, an aldolase and an aldo-keto reductase. Only the activity of the aldo-
304 keto reductase, YdjG, has been confirmed through reduction of methylglyoxal (20, 21).
305 Interestingly, a previous analysis of *E.coli* protein expression in germ-free mice showed
306 that YdjG was expressed 3.5-fold higher in the cecum than *in vitro* (22). Another gene
307 which has been studied in this operon, *ydjK*, may play a role in osmotolerance, showing
308 a 50% increased growth rate in high-salt media when overexpressed in *E. coli* (23). It is
309 not known whether methylglyoxal or osmotic stress can directly trigger transcription of
310 the *ydjLKJIHG* operon. However, methylglyoxal occurs in many foods and is also
311 produced by intestinal bacteria (24); it can also inhibit bacterial growth, suggesting a
312 possible motivation for expression of *ydjLKJIHG* in the gut.
313 Promoters derived from three unique Nissle 1917 operons (*ynfEFGH*, *torCAD*,
314 and *yeaR-yoaG*) showed robust memory response in the healthy mouse gut (Fig. 4D
315 and 4E). The *ynfEFGH* operon encodes a DMSO reductase which has also been shown
316 to reduce selenate (25, 26). It is activated by FNR in anaerobic conditions and
317 repressed by phosphorylated NarL in the presence of nitrate (19), which was further
318 confirmed by our *in vitro* tests (Fig. 4G).
319 Tuning of trigger sensitivity (e.g., by RBS modulation) is important for generating
320 responses to physiological conditions of interest and for successful application in
321 synthetic engineered circuits. As we observed, RBS tuning can be used to increase the
322 response of the ynfE promoter to as high as 100% in healthy mice (PAS816; Fig. 4F),

323 and to adjust the response to distinguish the inflamed gut state (PAS819; Fig. 5C).
324 Importantly, the sensors we identify can be used directly in downstream applications
325 with the memory circuit. This provides an engineering advantage over any responsive
326 genetic elements identified through analysis in their native context, for which
327 incorporation into synthetic circuits would routinely require additional optimization.
328 Inflammation leads to an increase in nitric oxide produced by the host, which
329 generates nitrate in the intestine (27). However, because the ynfE promoter is activated
330 by a decrease in nitrate, our results suggest that DSS-induced inflammation may lead to
331 lower levels of free nitrate available to *E. coli* NGF-1, possibly due to increased local
332 competition for nitrate via respiration by NGF-1 and other *Enterobacteriaceae*. This idea
333 is supported by our observation of increasingly higher NGF-1 bacterial loads in fecal
334 samples of DSS-treated mice (Fig. S4C and S4F), suggesting a bloom of *E. coli*—and
335 potentially other *Enterobacteriaceae* capable of nitrate respiration—correlated with
336 increasing duration of DSS treatment. This is consistent with previous descriptions of *E.*
337 *coli* experiencing a growth advantage due to anaerobic respiration of host-derived
338 nitrate (27). Thus, we hypothesize that PAS819 responds in DSS-treated mice
339 specifically through sensing inflammation-induced changes in its own
340 microenvironment.
341 The HTMS enables both the recording of transient signals and the amplification
342 of low-abundance signals through antibiotic selection. These features serve as a useful
343 complement to other techniques, such as meta-transcriptomic or -proteomic studies
344 which capture an instantaneous snapshot of total RNA or protein content. Screening of
345 genome-wide libraries increases the chances of discovery of new, uncharacterized

346 systems, while curating libraries to focus on a subset of sensors can allow greater fine-
347 tuning and increase the chances of identifying a response for the condition of interest.
348 Our use of the *E. coli* NGF-1 strain as a chassis allows robust colonization of the mouse
349 gut without requiring antibiotic maintenance, leading to retention of high bacterial loads
350 and high library complexity in fecal samples even after long periods in the gut.

351 An expanded arsenal of characterized sensors presents opportunities to
352 construct more complex disease-responsive circuits. For instance, the combination of
353 multiple redundant sensors would increase response accuracy under variable *in vivo*
354 conditions, while complementary sensors may allow "fingerprinting" of different disease
355 states. An exciting possibility is the use of more complex logic and signal processing
356 within a single engineered strain, which may sense multiple inputs and produce anti-
357 inflammatory, antimicrobial or other therapeutic proteins only when a precise set of
358 conditions is satisfied (2). Sensors responding differentially based on localization within
359 the intestine may create opportunities for more targeted drug delivery or for the
360 construction of new safety and containment mechanisms—another important
361 consideration in the deployment of engineered organisms.

362 The potential to engineer synthetic circuits into commensal gut bacteria is a
363 promising new approach to the management of intestinal disease. Synthetic biology is
364 just beginning to tap into the evolutionary breadth of capabilities found in natural
365 systems, and our method represents a practical means for expanding the toolkit of
366 useful sensors for *in vivo* application.

367

368 **MATERIALS AND METHODS**

369 **Media, culture conditions.** Unless otherwise mentioned, bacterial cultures were
370 grown at 37°C in LB broth or agar (10 g/L NaCl, 5 g/L yeast extract, 10 g/L tryptone).
371 Mixed liquid cultures (i.e., libraries) were grown in LBPS, which contains Peptone
372 Special (Sigma) instead of tryptone. To quantify memory response on indicator plates,
373 agar was supplemented with 60 µg/ml X-gal.

374 **High-throughput memory system (HTMS) construction.** The spectinomycin
375 resistance gene, *aadA*, was added downstream of the P_L promoter in the original
376 memory element (9) by overlap extension PCR and genomically integrated by λ Red
377 recombineering (28) into *E. coli* TB10 (29) between *mhpR* and *lacZ*, driving endogenous
378 *lacZ* as a memory-on reporter. From TB10, transfer into streptomycin-resistant *E. coli*
379 NGF-1 was by P1*vir* transduction.

380 **Biosensor strain and library construction.** All triggers were cloned into pDR07
381 (Fig. S2), a Tn7 transposon insertion plasmid derived from pGRG36 (12). BsaI sites
382 directly upstream of cIDN allow modular insertion of promoter–RBS sequences via
383 Golden Gate assembly (13) (Fig. 2A). Assembled trigger plasmids were electroporated
384 into PAS811. After recovery (90 min, 30°C in SOC medium) transformants were
385 selected overnight (30°C in LB-ampicillin (100 µg/ml)). Cultures were then back-diluted
386 1:100 into LB-chloramphenicol (25 µg/ml) + 0.1% arabinose to induce transposase
387 genes. After > 6 h at 30°C, temperature-sensitive pDR07 plasmids were cured from
388 integrants by 2x 1:100 back-dilution into LB-chloramphenicol and > 6 h growth at 42°C.
389 Plasmid loss was confirmed by restreaking on LB ampicillin agar.

390 For individual strains, post-cure cultures were plated on LB-chloramphenicol
391 agar and attTn7 integrations confirmed by PCR and Sanger sequencing. For pooled

392 libraries, library composition was confirmed by Illumina MiSeq sequencing of pooled
393 PCRs of trigger regions.

394 **Assessment of memory state by LacZ assay.** Cultures or fecal supernatants
395 containing memory bacteria were plated on agar plates containing streptomycin (200
396 mg/ml), chloramphenicol (34 mg/ml), and X-gal (60 mg/ml). The percentage of memory-
397 on colonies was assessed by counting blue (on) and white (off) colonies.

398 ***In vitro* induction.** Overnight liquid cultures were back-diluted 1:100 into fresh
399 media containing inducer, before 4 hours growth and plating on X-gal agar. For
400 induction in cecal contents, contents of ceca from three female SPF C57BL/6J mice and
401 suspended at 10% w/v in phospho-buffered saline (PBS). Suspensions were vortexed
402 90 sec and centrifuged for 3 min at 4300 rcf. The supernatant was recovered,
403 supplemented with 200 µg/ml streptomycin and used for growth of HTMS bacteria.

404 For anaerobic inductions, pre-reduced anaerobic medium was used, and growth
405 occurred in an anaerobic chamber (Coy Laboratory Products) under 7% H_2, 20% CO_2,
406 73% N_2.

407 ***In vivo* induction of strains and libraries.** The Harvard Medical School Animal
408 Care and Use Committee approved all animal protocols. Experiments were conducted
409 in female 7- to 14-week-old BALB/c (Charles River; MG1655 library) or C57BL/6J
410 (Jackson; Nissle 1917 library) mice. Before experiments, all mice were confirmed to be
411 absent of native streptomycin- and chloramphenicol-resistant flora. Food and water
412 were removed ~4 h before each gavage; water was replaced immediately, and food was
413 replaced < 2 h following gavage.

414 One day prior to bacterial gavage, mice were provided streptomycin (20 mg in
415 PBS) by oral gavage. The next day, overnight cultures of memory strains or libraries
416 were washed once, then diluted 10-fold in PBS and administered by gavage (100µl;
417 ~10^7 bacteria/mouse).
418 Gavage suspension and fecal samples were plated to track bacterial load and,
419 for individual strains, to assess memory state. Libraries were processed according to
420 the post-exposure processing protocol below. To plate fecal bacteria, samples were
421 suspended at 100 mg/ml in PBS, vortexed 5 min, and centrifuged 20 min at 4 rcf to
422 obtain fecal supernatant.
423 For inflammation experiments, water containing 4% DSS (36,000-50,000 M.W.;
424 MP Biomedicals 160110) was substituted 2 h after bacteria administration. Mice were
425 dissected at the end of the experiment to measure colon length.
426 **Post-exposure library processing.** Fecal supernatant or *in vitro* culture was
427 diluted 1:100 into LBPS-chloramphenicol (25 µg/ml) to achieve ~10^6 CFU/ml.
428 Concurrently, an overnight culture of the positive normalization strain, PAS812 was
429 back-diluted 1:100 into LBPS-chloramphenicol. Cultures were grown 4 h, or until OD_{600}
430 ~1. PAS812 OD_{600} was adjusted to match the library culture, then diluted 1:1000 into
431 the library culture. The resulting mix was back-diluted 1:1000 into 50 ml LBPS-
432 chloramphenicol, and immediately split into two 25 ml volumes. Spectinomycin (50
433 µg/ml) was added to one culture, and both were grown overnight before centrifugation
434 to collect bacterial pellets, which were stored at -80°C.
435 **Library sequencing and odds ratio calculation.** Genomic DNA was extracted
436 from frozen cell pellets using a Qiagen DNEasy Blood & Tissue Kit. Using genomic DNA

437 as a template, trigger regions from HTMS libraries were amplified by PCR and sheared
438 with a Covaris M220 ultrasonicator to 200-600 bp fragments. Sheared products were
439 prepared using the New England Biolabs NEBNext Ultra II Prep Kit and sequenced by
440 Illumina MiSeq.

441 Raw reads were trimmed using Trimmomatic 0.36 (30) and aligned to a
442 reference file (Data Sets S4 and S5 for MG1655 and Nissle 1917 libraries, respectively)
443 using BWA mem 0.7.8 (31). The number of uniquely-mapped reads for each trigger was
444 counted.

445 Odds ratio is expressed as $(T_{x\text{-spect}}/PNS_{spect})/(T_x/PNS)$, where T_x and $T_{x\text{-spect}}$ are
446 the number of mapped reads for a particular trigger in the untreated and spectinomycin-
447 treated culture, respectively, and PNS and PNS_{spect} are the number of mapped reads for
448 the positive normalization strain (PAS812) in the untreated and spectinomycin-treated
449 culture, respectively. Triggers with < 5 reads in the gavage suspension were discarded,
450 unless they registered > 20 reads at any subsequent timepoint. For each pair of
451 untreated and spectinomycin-treated cultures (from a single fecal sample), odds ratios
452 were calculated for each trigger with ≥ 5 reads in the untreated culture. Statistical
453 significance was assessed with a one-tailed Fisher's exact test (H_0: odds ratio = 0.02;
454 H_a: odds ratio > 0.02). The odds ratio calculation compares each trigger only with itself
455 (between spectinomycin-treated and untreated cultures), normalizing any sequencing
456 length bias between triggers. It also normalizes to the positive normalization strain
457 (PAS812) in each sample, negating read depth disparities between samples.
458

459 **ACKNOWLEDGEMENTS**

We thank Bryan Hsu, Andrew Verdegaal and Joseph Paulson for helpful discussions. A.D.N. was supported by the National Science Foundation Graduate Research Fellowship (DGE1144152 & DGE1745303). S.N.N. was supported by the Ruth L. Kirschstein Individual Postdoctoral NRSA F32 (F32 DK112640-03). D.T.R. was supported by the Human Frontier Science Program Long-Term Fellowship and the NHMRC/RG Menzies Early Career Fellowship from the Menzies Foundation through the Australian National Health and Medical Research Council.

Author contributions: A.D.N., D.T.R., J.J.B, S.N.N., and P.A.S. designed experiments. A.D.N., S.N.N., J.J.B and D.T.R. constructed libraries. A.D.N., S.N.N., D.T.R, D.T., N.N., M.J.N., and M.C.I. performed in vitro characterization. A.D.N. and D.T.R. performed mouse experiments. A.D.N., J.J.B. and D.T.R. performed and analyzed library sequencing. A.D.N., D.T.R. and P.A.S. wrote the manuscript.

472 **REFERENCES**

473 1. Ozdemir T, Fedorec AJH, Danino T, Barnes CP. 2018. Synthetic Biology and
474 Engineered Live Biotherapeutics: Toward Increasing System Complexity. Cell Syst
475 7:5–16.

476 2. Riglar DT, Silver PA. 2018. Engineering bacteria for diagnostic and therapeutic
477 applications. Nat Rev Microbiol 16:214.

478 3. Riglar DT, Giessen TW, Baym M, Kerns SJ, Niederhuber MJ, Bronson RT, Kotula
479 JW, Gerber GK, Way JC, Silver PA. 2017. Engineered bacteria can function in the
480 mammalian gut long-term as live diagnostics of inflammation. Nat Biotechnol
481 35:nbt.3879.

482 4. Daeffler KN-M, Galley JD, Sheth RU, Ortiz-Velez LC, Bibb CO, Shroyer NF, Britton
483 RA, Tabor JJ. 2017. Engineering bacterial thiosulfate and tetrathionate sensors for
484 detecting gut inflammation. Mol Syst Biol 13:923.

485 5. Mimee M, Nadeau P, Hayward A, Carim S, Flanagan S, Jerger L, Collins J,
486 McDonnell S, Swartwout R, Citorik RJ, Bulović V, Langer R, Traverso G,
487 Chandrakasan AP, Lu TK. 2018. An ingestible bacterial-electronic system to
488 monitor gastrointestinal health. Science 360:915–918.

489 6. Hwang IY, Koh E, Wong A, March JC, Bentley WE, Lee YS, Chang MW. 2017.
490 Engineered probiotic Escherichia coli can eliminate and prevent Pseudomonas
491 aeruginosa gut infection in animal models. Nat Commun 8:ncomms15028.

492 7. Mao N, Cubillos-Ruiz A, Cameron DE, Collins JJ. 2018. Probiotic strains detect and
493 suppress cholera in mice. Sci Transl Med 10:eaao2586.

494 8. Rediers H, Rainey PB, Vanderleyden J, Mot RD. 2005. Unraveling the Secret Lives
495 of Bacteria: Use of In Vivo Expression Technology and Differential Fluorescence
496 Induction Promoter Traps as Tools for Exploring Niche-Specific Gene Expression.
497 Microbiol Mol Biol Rev 69:217–261.

498 9. Kotula JW, Kerns SJ, Shaket LA, Siraj L, Collins JJ, Way JC, Silver PA. 2014.
499 Programmable bacteria detect and record an environmental signal in the
500 mammalian gut. Proc Natl Acad Sci 111:4838–4843.

501 10. Noman N, Inniss M, Iba H, Way JC. 2016. Pulse Detecting Genetic Circuit – A New
502 Design Approach. PLOS ONE 11:e0167162.

503 11. Gimble FS, Sauer RT. 1985. Mutations in bacteriophage lambda repressor that
504 prevent RecA-mediated cleavage. J Bacteriol 162:147.

505 12. McKenzie GJ, Craig NL. 2006. Fast, easy and efficient: site-specific insertion of
506 transgenes into Enterobacterial chromosomes using Tn7 without need for selection
507 of the insertion event. BMC Microbiol 6:39.

508 13. Engler C, Kandzia R, Marillonnet S. 2008. A One Pot, One Step, Precision Cloning
509 Method with High Throughput Capability. PLOS ONE 3:e3647.

510 14. Mutalik VK, Guimaraes JC, Cambray G, Lam C, Christoffersen MJ, Mai Q-A, Tran
511 AB, Paull M, Keasling JD, Arkin AP, Endy D. 2013. Precise and reliable gene

512 expression via standard transcription and translation initiation elements. Nat
513 Methods 10:354–360.

514 15. Ziesack M, Karrenbelt MAP, Bues J, Schaefer E, Silver P, Way J. 2018.
515 Escherichia coli NGF-1, a Genetically Tractable, Efficiently Colonizing Murine Gut
516 Isolate. Microbiol Resour Announc 7:e01416-18.

517 16. Zaslaver A, Bren A, Ronen M, Itzkovitz S, Kikoin I, Shavit S, Liebermeister W,
518 Surette MG, Alon U. 2006. A comprehensive library of fluorescent transcriptional
519 reporters for Escherichia coli. Nat Methods 3:623–628.

520 17. Hughes ER, Winter MG, Duerkop BA, Spiga L, Furtado de Carvalho T, Zhu W,
521 Gillis CC, Büttner L, Smoot MP, Behrendt CL, Cherry S, Santos RL, Hooper LV,
522 Winter SE. 2017. Microbial Respiration and Formate Oxidation as Metabolic
523 Signatures of Inflammation-Associated Dysbiosis. Cell Host Microbe 21:208–219.

524 18. Winter SE, Lopez CA, Bäumler AJ. 2013. The dynamics of gut-associated microbial
525 communities during inflammation. EMBO Rep 14:319–327.

526 19. Xu M, Busby SJW, Browning DF. 2009. Activation and Repression at the
527 Escherichia coli ynfEFGHI Operon Promoter. J Bacteriol 191:3172–3176.

528 20. Di Luccio E, Elling RA, Wilson DK. 2006. Identification of a novel NADH-specific
529 aldo-keto reductase using sequence and structural homologies. Biochem J
530 400:105–114.

531 21. Jain R, Yan Y. 2011. Dehydratase mediated 1-propanol production in metabolically
532 engineered Escherichia coli. Microb Cell Factories 10:97.

533 22. Vogel-Scheel J, Alpert C, Engst W, Loh G, Blaut M. 2010. Requirement of Purine
534 and Pyrimidine Synthesis for Colonization of the Mouse Intestine by Escherichia
535 coli. Appl Environ Microbiol 76:5181–5187.

536 23. Winkler JD, Garcia C, Olson M, Callaway E, Kao KC. 2014. Evolved Osmotolerant
537 Escherichia coli Mutants Frequently Exhibit Defective *N* -Acetylglucosamine
538 Catabolism and Point Mutations in Cell Shape-Regulating Protein MreB. Appl
539 Environ Microbiol 80:3729–3740.

540 24. Zhang S, Jiao T, Chen Y, Gao N, Zhang L, Jiang M. 2014. Methylglyoxal Induces
541 Systemic Symptoms of Irritable Bowel Syndrome. PLOS ONE 9:e105307.

542 25. Jones SA, Gibson T, Maltby RC, Chowdhury FZ, Stewart V, Cohen PS, Conway T.
543 2011. Anaerobic Respiration of Escherichia coli in the Mouse Intestine. Infect
544 Immun 79:4218–4226.

545 26. Guymer D, Maillard J, Sargent F. 2009. A genetic analysis of in vivo selenate
546 reduction by Salmonella enterica serovar Typhimurium LT2 and Escherichia coli
547 K12. Arch Microbiol Berl 191:519–28.

548 27. Winter SE, Winter MG, Xavier MN, Thiennimitr P, Poon V, Keestra AM, Laughlin
549 RC, Gomez G, Wu J, Lawhon SD, Popova IE, Parikh SJ, Adams LG, Tsolis RM,
550 Stewart VJ, Bäumler AJ. 2013. Host-Derived Nitrate Boosts Growth of E. coli in the
551 Inflamed Gut. Science 339:708–711.

552 28. Datsenko KA, Wanner BL. 2000. One-step inactivation of chromosomal genes in
553 Escherichia coli K-12 using PCR products. Proc Natl Acad Sci 97:6640–6645.

554 29. Johnson JE, Lackner LL, Hale CA, de Boer PAJ. 2004. ZipA Is Required for
555 Targeting of DMinC/DicB, but Not DMinC/MinD, Complexes to Septal Ring
556 Assemblies in Escherichia coli. J Bacteriol 186:2418–2429.

557 30. Bolger AM, Lohse M, Usadel B. 2014. Trimmomatic: a flexible trimmer for Illumina
558 sequence data. Bioinforma Oxf Engl 30:2114–2120.

559 31. Li H. 2013. Aligning sequence reads, clone sequences and assembly contigs with
560 BWA-MEM. ArXiv13033997 Q-Bio.

561

562 # TABLES

563 **TABLE 1** Key memory strains used in this study.

Strain	E. coli strain	Memory	Trigger Promoter/RBS	Trigger Gene	Source
PAS132	K-12 MG1655	original	tet	*cro*	(9)
PAS133	NGF-1	original	tet	*cro*	(9)
PAS807	K-12 MG1655	original	tet	*cIDN*	this study
PAS808	NGF-1	original	tet	*cIDN*	this study
PAS809	NGF-1	original	tet	*cIDN*	this study
PAS810	NGF-1	HTMS	tet	*cIDN*	this study
PAS811	NGF-1	HTMS	-	-	this study
PAS812	NGF-1	HTMS	fabR	*cIDN*	this study
PAS813	NGF-1	HTMS	ydiL	*cIDN*	this study
PAS814	NGF-1	HTMS	ydjL	*cIDN*	this study
PAS815	NGF-1	HTMS	-	*cIDN*	this study
PAS816	NGF-1	HTMS	ynfE15	*cIDN*	this study
PAS817	NGF-1	HTMS	yeaRWT	*cIDN*	this study
PAS818	NGF-1	HTMS	ynfEWT	*cIDN*	this study
PAS819	NGF-1	HTMS	ynfE17	*cIDN*	this study

564

565 **FIGURES**

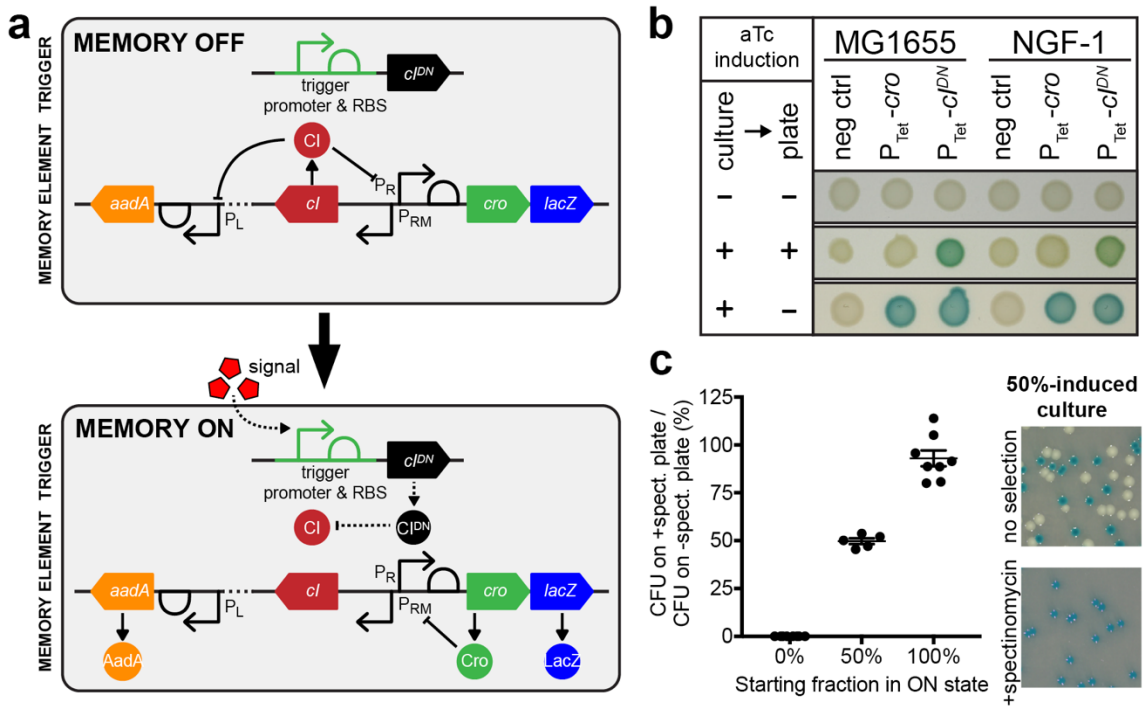

566

567 **FIG 1** Design of a High-Throughput Memory System (HTMS). (A) HTMS circuit design
568 in memory-off and memory-on states. (B) Comparison of memory element induction
569 with *cro* and *cIDN* triggers illustrates differences in induction dynamics. Control and
570 memory strains with P_{tet} triggers (PAS132, PAS133, PAS807, PAS808) were grown in
571 liquid media, then spotted on indicator plates, each with or without aTc induction (100
572 ng/ml). (C) Selection of memory-on HTMS with spectinomycin. Memory-off, memory-on,
573 and 50-50 mixed cultures of PAS810 were plated on indicator plates with or without
574 spectinomycin (inset photo). Graph shows comparison of CFU counts between
575 +spectinomycin and -spectinomycin plates. Error bars represent SE of eight biological
576 replicates (for 0% and 100%) and five biological replicates (for 50%).

577

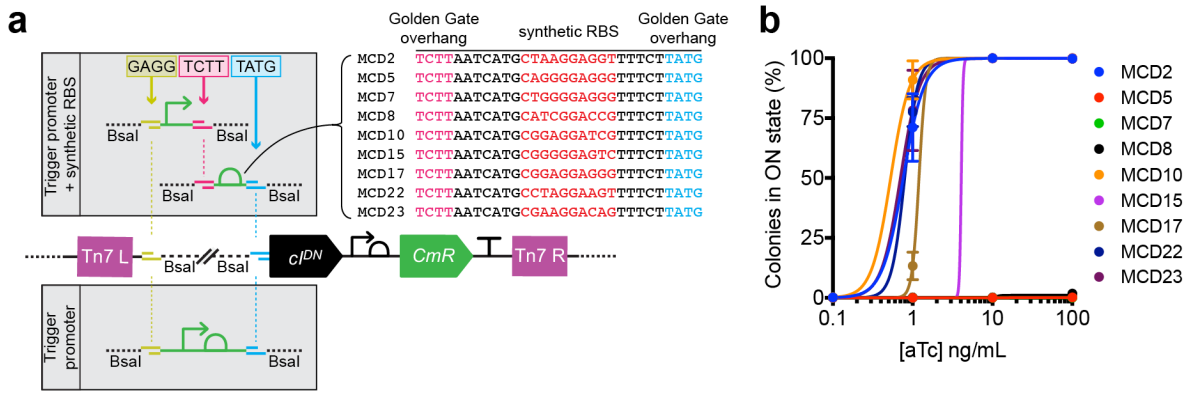

FIG 2 Tuning of trigger sensitivity is achieved through modular incorporation of RBS variants. (A) Strategy for insertion of trigger promoter and RBS variants (14) by Golden Gate assembly (13) into a Tn7 transposon plasmid containing the *cIDN* gene (Fig. S2). (B) Response curves for RBS variants of a Ptet-*cIDN* trigger in the HTMS chassis strain PAS811 induced with varying concentrations of aTc. Memory response was assessed by plating of bacteria on indicator plates after induction with aTc in liquid culture. Error bars represent SE of three biological replicates.

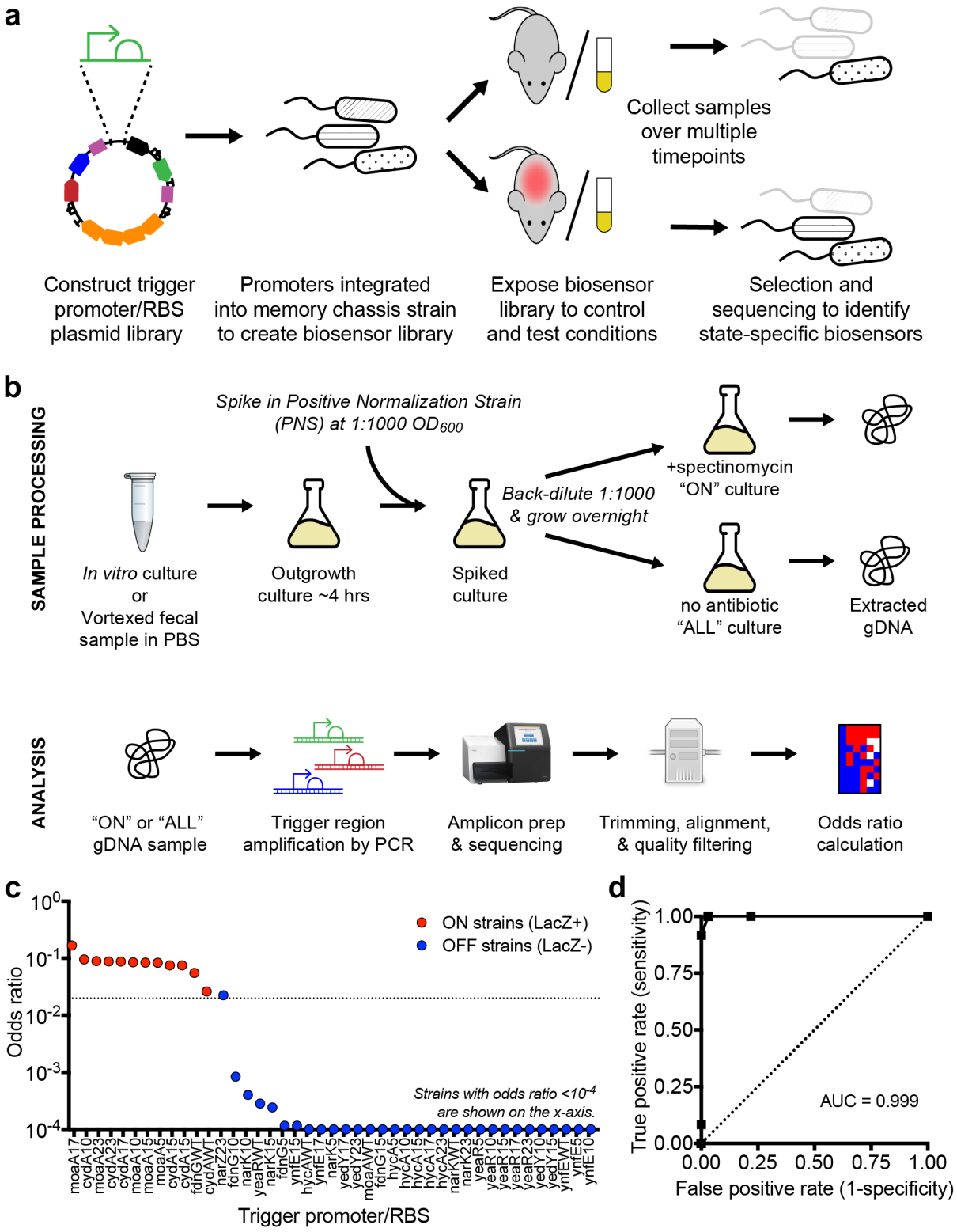

FIG 3 Biosensor library screening and analysis. (A) Libraries were constructed as plasmids, integrated into the genome at single copy, and screened as a pool for

590 differential response to growth in control and test environments. (B) Post-exposure
591 library sample processing, selection for memory-on strains, sequencing and analysis.
592 The consistently memory-on positive normalization strain (PAS812) is spiked in prior to
593 spectinomycin selection and used for calculation of odds ratios. (C) Calculated odds
594 ratio from *in vitro* pooled growth in LB medium vs. memory state assessed by plating
595 individual library strains on LB agar indicator plates. 44 strains subsampled from the
596 Nissle 1917 library were tested. The on-off odds ratio cutoff used in the subsequent *in*
597 *vivo* screens (0.02) is indicated by the dotted line. (D) ROC curve for varying odds ratio
598 cutoffs as an indicator of memory state.

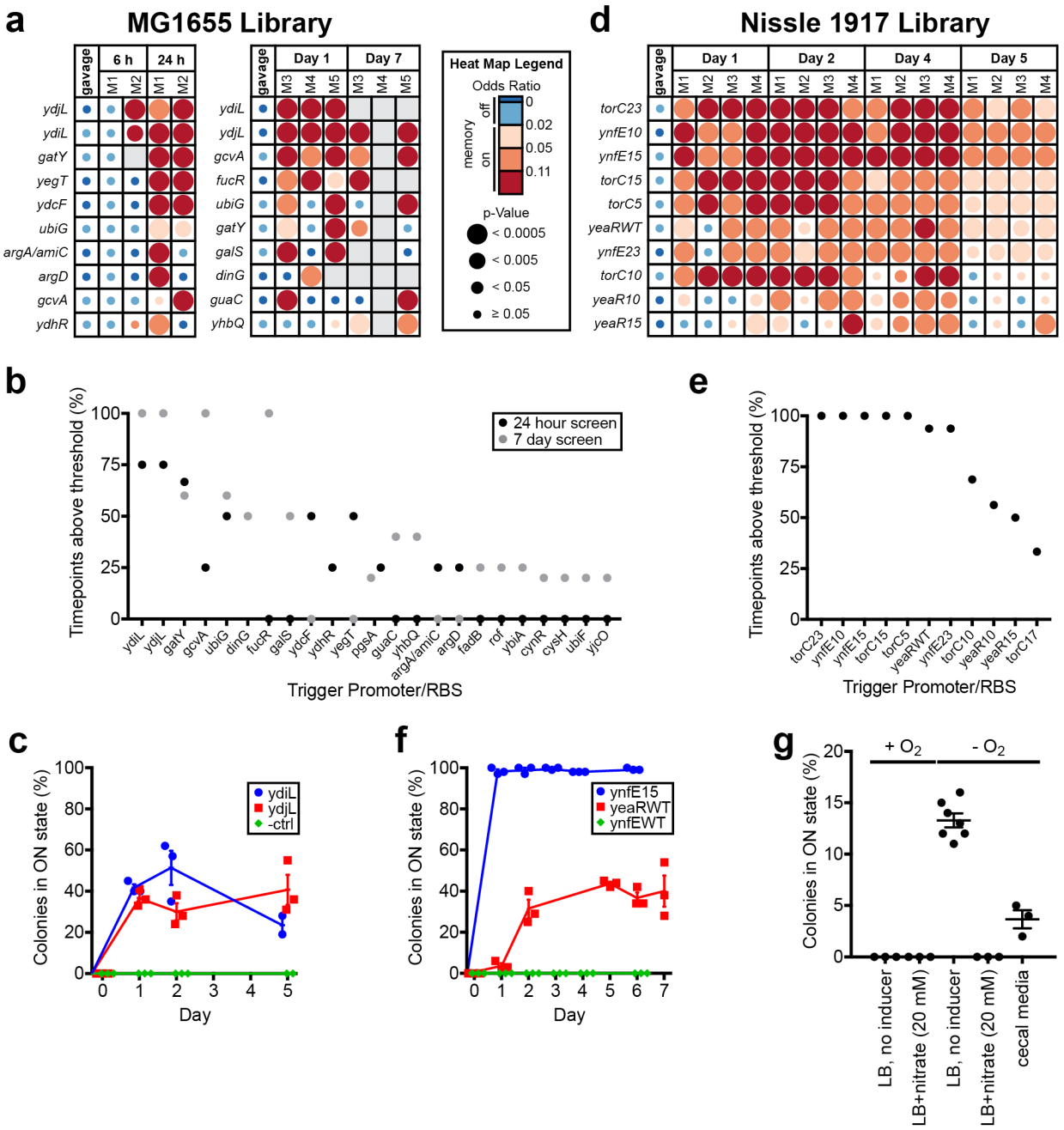

FIG 4 Library screening and individual sensor testing identifies biosensors of the *in vivo* gut environment. (A) Screen of MG1655 library in BALB/c mice over one day (left; n = 2) and over seven days (right; n = 3). Odds ratio heat maps of the top 10 hits sorted by percentage of positive timepoints (odds ratio ≥ 0.02 and $p < 0.05$) over the course of the experiment. Blank spaces on heat maps represent insufficient sequencing coverage.

605 See Data Set S1 and S2 for full results. (B) Percentage of positive timepoints (odds
606 ratio $\geq$ 0.02 and $p < 0.05$) for all positive hits from two MG1655 library screens (top 10
607 shown in Fig. 4A). (C) Response of individual strains from MG1655 library in healthy
608 mice. HTMS strains containing triggers ydiL (PAS813), ydjL (PAS814) and an empty
609 trigger (PAS815) were administered as monocultures to BALB/c mice (n = 3). Memory
610 response was assessed by plating of HTMS bacteria recovered from fecal samples on
611 indicator plates. Error bars represent SE. (D) Screen of Nissle 1917 library in C57BL/6J
612 mice (n = 4) over five days. Odds ratio heat map of the top 10 hits sorted by percentage
613 of positive timepoints (odds ratio $\geq$ 0.02 and $p < 0.05$) over the course of the
614 experiment. Blank spaces on heat map represent insufficient sequencing coverage. See
615 Data Set S3 for full results. (E) Percentage of positive timepoints (odds ratio $\geq$ 0.02 and
616 $p < 0.05$) for all hits from Nissle 1917 library screen in healthy mice (top 10 shown in
617 Fig. 4D). (F) Response of individual strains from Nissle 1917 library in healthy mice.
618 HTMS strains containing the ynfE trigger with MCD15 (PAS816), the yeaR trigger with
619 its WT RBS (PAS817) and the ynfE trigger with its WT RBS (PAS818) were
620 administered as monocultures to C57BL/6J mice (n = 3). Memory response was
621 assessed by plating of HTMS bacteria recovered from fecal samples on indicator plates.
622 Error bars represent SE. (G) Response of the ynfE15 trigger strain (PAS816) to *in vitro*
623 growth in rich media with and without 20 mM nitrate, with and without oxygen, and in the
624 presence of mouse cecum fluid medium. Memory response was assessed by plating on
625 indicator plates after growth in liquid culture. Error bars represent SE. (n = 7 for $-O_2$, LB,
626 no inducer condition; n = 3 for all other conditions.)

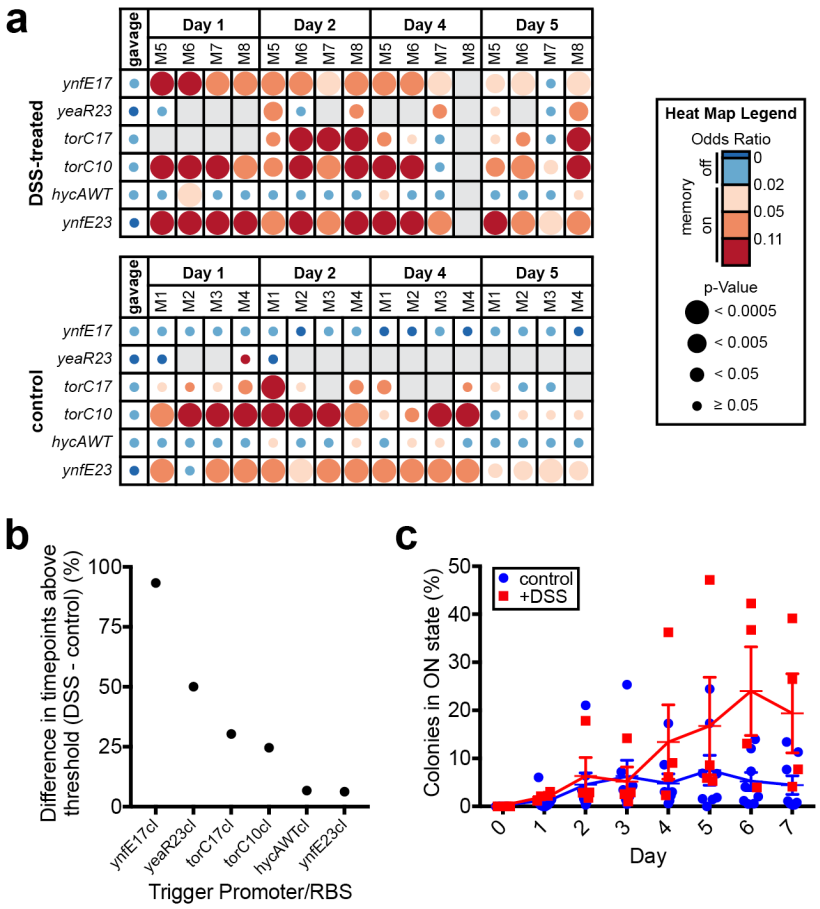

FIG 5 Library screening and individual sensor testing identifies biosensors with increased response during inflammation. (A) Screen of Nissle 1917 library in DSS-treated C57BL/6J mice (n = 4) over five days and comparison with results of previous screen in healthy C57BL/6J mice (n = 4; control group; also see Fig. 4D and 4E). To identify sensors responding more strongly to the inflamed state, the fraction of timepoints registering memory-on (odds ratio ≥ 0.02 and $p < 0.05$) in the control group was subtracted from the fraction in the DSS-treated group for each strain in the library, and strains were sorted according to the greatest difference between the two groups. Odds ratio heat map of the six strains registering a positive difference between the two groups is shown. Blank spaces on heat map represent insufficient sequencing coverage. See Data Set S3 for full results. (B) Differences in percentage of positive

timepoints (odds ratio ≥ 0.02 and $p < 0.05$) between DSS-treated and control group mice for strains showing a positive difference between the two groups (heat map shown in Fig. 5A). (C) Response of HTMS strain containing the ynfE trigger with MCD17 (PAS819) in DSS-treated mice (n = 4) and healthy mice (n = 8). Memory response was assessed by plating of HTMS bacteria recovered from fecal samples on indicator plates. Error bars represent SE.

645 ## SUPPLEMENTAL MATERIAL LEGENDS

646

647 **FIG S1** (A) Original memory circuit (9) in memory-off and memory-on states. (B)
648 Response curves of P_{tet}-*cIDN* trigger original memory (PAS809) & an aadA memory
649 strain (PAS810), induced with varying concentrations of aTc. Memory response was
650 assessed by plating on indicator plates after induction with aTc in liquid culture. Error
651 bars represent SE of three biological replicates.

652

653 **FIG S2** Plasmid map of Tn7 transposon trigger integration plasmid, pDR07, containing
654 BsaI sites upstream of *cIDN* gene for modular insertion of trigger promoter and RBS
655 variants via Golden Gate assembly (see Fig. 2A). Tn7 left and right attachment sites are
656 shown in pink.

657

658 **FIG S3** Heatmap for hits from Nissle 1917 library screen in healthy C57BL/6J mice (Fig.
659 4D and 4E), when screened in C57BL/6J mice treated with 4% w/v DSS in water. Blank
660 spaces on heat map represent insufficient sequencing coverage. See Data Set S3 for
661 full heat map.

662

663 **FIG S4** Body weights, CFU counts, and colon lengths of mice in Nissle 1917 library
664 screen and ynfE17 (PAS819) biosensor strain validation experiments. All error bars
665 represent SE. (A) Percentage of starting body weight for DSS-treated (n = 4) and
666 healthy control (n = 4) mice used in Nissle 1917 library screens. (B) Colon lengths at
667 dissection for DSS-treated (n = 4) and healthy control (n = 4) mice used in Nissle 1917

library screens. (C) CFU of HTMS bacteria in fecal samples of DSS-treated (n = 4) and healthy control (n = 4) mice used in Nissle 1917 library screens. (D) Percentage of starting body weight for DSS-treated (n = 4) and healthy control (n = 8) mice used in PAS819 validation experiment. (E) Colon lengths at dissection for DSS-treated (n = 4) and healthy control (n = 8) mice used in PAS819 validation experiment. (F) CFU of HTMS bacteria in fecal samples of DSS-treated (n = 4) and healthy control (n = 8) mice used in PAS819 validation experiment.

DATA SET S1. Screen of MG1655 library in 2 BALB/c mice over 24 hours (full heat map corresponding to Fig. 4A). See Fig. 4 for heat map legend.

DATA SET S2. Screen of MG1655 library in 3 BALB/c mice over seven days (full heat map corresponding to Fig. 4B). See Fig. 4 for heat map legend.

DATA SET S3. Screen of Nissle 1917 library in 8 C57BL/6J mice over five days, with and without DSS treatment (full heat map corresponding to Fig. 4D and 5A). See Fig. 4 or Fig. 5 for heat map legend.

DATA SET S4. Sequence reference file (fasta) for aligning MG1655 library reads.

DATA SET S5. Sequence reference file (fasta) for aligning Nissle 1917 library reads.